ChemComm

Accepted Manuscript

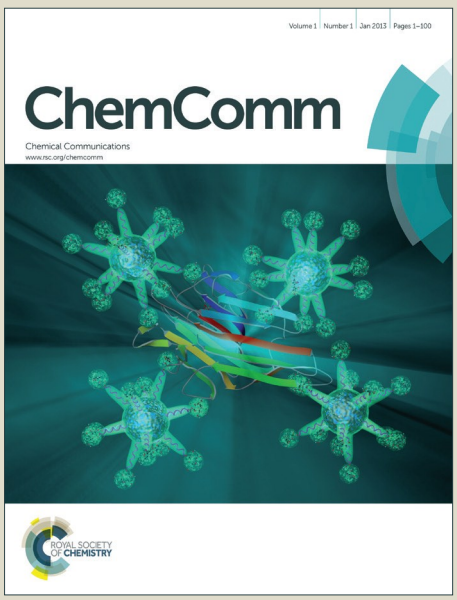

ROYAL SOCIETY OF CHEMISTRY

www.rsc.org/chemcomm

ChemComm

COMMUNICATION

Isotope effect analyses provide evidence for an altered transition state for RNA 2'-*O*-transphosphorylation catalyzed by Zn^{2+}

Received 00th January 20xx,
Accepted 00th January 20xx

DOI: 10.1039/x0xx00000x

www.rsc.org/

Shuming Zhang[a], Hong Gu[a], Haoyuan Chen[b], Emily Strong[a], Edward W. Ollie[a], Daniel Kellerman[a], Danni Liang[a], Masaru Miyagi[c], Vernon E. Anderson[a], Joseph A. Piccirilli[d], Darrin M. York[b] and Michael E. Harris[a]

Solvent D_2O and ^{18}O kinetic isotope effects on RNA 2'-*O*-transphosphorylation catalyzed by Zn^{2+} demonstrate an altered transition state relative to specific base catalysis. A recent model from DFT calculations involving inner sphere coordination to the non-bridging and leaving group oxygens is consistent with the data.

Divalent ions are essential cofactors in the active sites of many phosphoryl transferases[1-6]. Although experimental information on how metal ions alter transition state (TS) structure is limited, the available data show effects can be quite large[1, 2]. Non-enzymatic model reactions offer the potential into address basic questions about the roles of metal ions in biological catalysis[1, 2, 7-11]. Such information can be useful to help guide the design of artificial enzymes[12, 13]. RNA cleavage by 2'-*O*-transphosphorylation is a useful system to explore the roles of metal ions in phosphoryl transfer catalysis because this reaction is catalyzed non-enzymatically by divalent ions[10, 14], by organometallic compounds[12, 13], as well as by ribonucleases including ribozymes[15, 16].

RNA 2'-*O*-transphosphorylation with displacement of the 5'O and formation of a 2',3'-cyclic phosphate is catalyzed by both acids and bases and the mechanisms of these reactions are well studied[8, 11, 17]. Thus, they provide contrasting examples for understanding RNA strand cleavage by divalent metals. Base catalysis involves equilibrium deprotonation of the 2'O nucleophile followed by nucleophilic attack. The mechanism is concerted via a late (product-like), anionic TS (Fig. 1A)[8, 18, 19]. Acid catalysis proceeds via a two-step mechanism involving the formation of a phosphorane intermediate in which one or both of the non-bridging oxygens may be protonated[8, 20]. Pseudorotation of the intermediate results in formation of 2',5' isomerization products that are characteristic of the two-step mechanism of acid catalysis[8].

The catalysis of RNA transesterification by metal ions and organometallic compounds have also been the subject of intensive study because of the importance of divalent metal ion cofactors in enzymes and potential application in synthetic catalysts[9, 10, 12, 14, 21]. The pH dependences of the rate constants for RNA cleavage reactions catalyzed by metal ions are typically consistent with base catalysis. Often an apparent pK_a consistent with titration of metal coordinated water molecules is also observed. Increasing acidity of metal coordinated aquo ligands generally correlates with a higher degree of rate enhancement. For displacement of basic alkyl groups like the 5'O of ribose, catalysis by metal ions and metal ion complexes can result in a decrease in β_{LG} reflecting a decrease in charge accumulation on the leaving group in the TS[9, 22]. Possible catalytic interactions involving divalent ions consistent with the available data include electrostatic stabilization of an anionic TS, inner sphere coordination of the nucleophile and leaving groups, and Brønsted acid/base catalysis involving coordinated water molecules[3-5] (Fig. 1B).

However, the precise modes of metal ion catalysis in both solution and enzyme reactions remain difficult to distinguish experimentally. This challenge is compounded now that recent biophysical and computational studies indicate that effects of metal ion catalysis on TS structure depend on the pKa of the leaving group, as well as and the number and type of metal ions involved in catalysis[9, 21]. Kinetic isotope effect analyses can provide a valuable experimental method for distinguishing differences in ground state and transition state bonding[23-30]. Such experimental data is critical for evaluating models of metal ion catalysis derived from computation. Therefore, we measured the ^{18}O KIEs on the 2'O nucleophile ($^{18}k_{NUC}$) and 5'O leaving group ($^{18}k_{LG}$) oxygens and the non-bridging phosphoryl oxygen ($^{18}k_{NPO}$) as well as solvent D_2O effects for RNA 2'-*O*-transphosphorylation reactions of uridylyl-3'-guanosine (5'-UpG-3', UpG) catalyzed by Zn^{2+} and by specific base.

Consistent with previous results[22], Zn^{2+} accelerates 2'-*O*-transphosphorylation of the dinucleotide UpG to yield uridine-2',3'-cyclic-monophosphate (2',3'-cUMP) and guanosine (Fig. S1). The dependence of the observed rate constant on Zn^{2+} concentration shows saturation and suggests two or more metal ions are involved in catalysis (Fig. S2), although, conclusive interpretation is complicated by the potential for changes in Zn^{2+} speciation at higher concentration. Accumulation of a 2',5' isomerization

[a] Department of Biochemistry, Case Western Reserve University School of Medicine, Cleveland, OH 44106.
[b] Center for Integrative Proteomics Research, BioMaPS Institute for Quantitative Biology and Department of Chemistry and Chemical Biology, Rutgers University Piscataway, NJ 08854.
[c] Case Center for Proteomics and Bioinformatics, Case Western Reserve University, Cleveland, OH, 44106.
[d] Department of Chemistry and Departent of Biochemistry and Molecular Biology, The University of Chicago, Chicago, IL 60637

Electronic Supplementary Information (ESI) available: [details of any supplementary information available should be included here]. See DOI: 10.1039/x0xx00000x

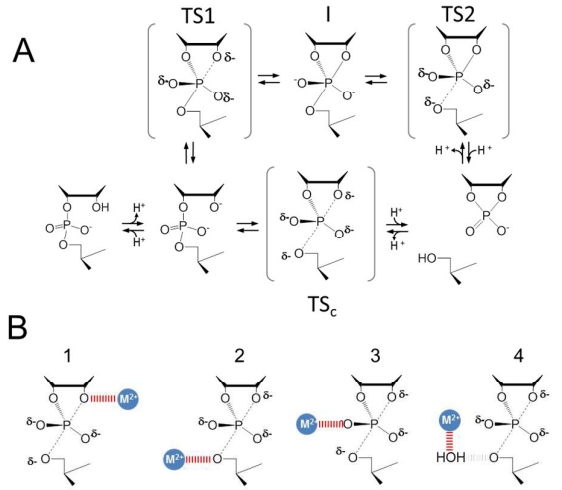

Fig. 1. A. Mechanisms of RNA 2'-*O*-transphosphorylation. Specific base catalysis involves equilibrium deprotonation of the 2'O resulting in a 2' oxyanion that acts as a nucleophile attacking the adjacent phosphoryl group. Experimental and computational data support a mechanism that involves a late TS (similar to TS2). Acid catalysis proceeds via a stepwise mechanism shown in the top pathway resulting in the formation of a stable phosphorane intermediate. The intermediate shown here is anionic for simplicity, however, in the acid mechanism this intermediate is protonated on one or more of the non-bridging oxygens. The potential formation of 2',5' diester products resulting from isomerization are also omitted for clarity. **B.** Proposed metal ion catalytic modes involving interactions with anionic TSs for RNA cleavage. Potential modes include interactions with the 2'O nucleophile (1), 5'O leaving group (2), and non-bridging oxygen (3). These interactions can involve direct coordination (1-3), H-bonding or transfer (4)

product is not observed, thus, a mechanism similar to acid catalysis involving the formation of a stable phosphorane is unlikely. Importantly, the log-linear dependence of the rate constant for Zn^{2+} catalysis on pH is consistent with either a general or specific base mechanism as reported previously (Fig. S3)[7, 14].

To gain information on whether Zn^{2+} catalysis alters the transition state by transfer of protons in the TS, we employed proton inventory analysis[31, 32]. This approach measures the dependence of the observed rate constant on the fraction D_2O in reactions containing mixtures of H_2O and D_2O. These data may be used to evaluate alternative models for the number of exchangeable protons that contribute to the observed SKIE and estimate the magnitude of the effect from each site (φ values). Both Zn^{2+} catalysis and specific base catalysis show similar, large normal SKIEs ($^{D}k_{OH}$ = 7.7 ± 0.9 and $^{D}k_{Zn}$ = 13.2 ± 0.5). A linear model for one titratable group affected by H/D substitution can fit the data (Fig. 2, red line), however, non-linear residuals makes this model unlikely. Models for Zn^{2+} transition state stabilization have proposed general acid catalysis involving a metal coordinated water or hydronium ion[21, 22]. In this mechanism the ΔpK_a of +0.85 in D_2O for the metal coordinated water would increase the concentration of the active form of the catalyst. This effect in turn would impart an inverse (k_{H2O}/k_{D2O} < 1) value of φ^R of *ca*. 0.14. That is, the reaction would be 7-fold faster in D_2O compared to H_2O. Such a large inverse effect would have to be more than offset by the presence of large normal fractionation factors in order to result in the >10-fold slower rate constant that is experimentally observed in D_2O. The presence of both normal and inverse φ values would result in an arch-shaped proton inventory, which is not observed experimentally (Fig. 2, blue line).

The proton inventories for both reactions are consistent with two normal fractionation factors: a large equilibrium effect due differences in 2'O solvation in the ground state ($1/\varphi^R$ ~ 0.2) and a second normal contribution of lower magnitude (φ^T ~ 0.4) observed in previous SKIE analyses of RNA cleavage (Fig. 2, black line) and attributed to differences in TS solvation. Proton inventory analyses, however, are known to have limited ability to distinguish models involving more than two exchangeable protons[31, 32]. Nonetheless, a simple interpretation is that there is little change in the number or contribution of catalytic modes involving proton transfer in the presence of the Zn^{2+} catalyst.

To better understand the effects of metal ion catalysis on O-P bonding we measured ^{18}O KIEs for Zn^{2+} catalyzed RNA transesterification. Heavy atom ^{18}O KIEs arise due to differences in

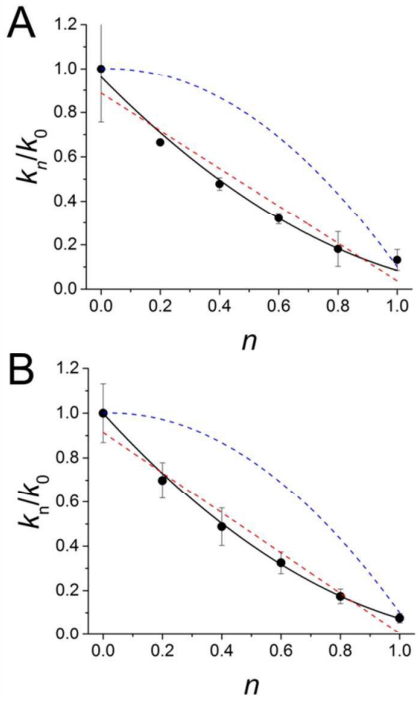

Fig. 2. Proton inventory of specific base (**A**) and Zn^{2+}-catalyzed (**B**) RNA 2'-*O*-transphosphorylation. The data are fit to a linear function or to the Gross-Butler equation (Eq. 3, ESI). The red dashed line represents a model for one normal fractionation factor of (φ^T = 0.14). The blue dashed line a simulation using Eq. 3 for a model involving acid catalysis in which there is a modest inverse fractionation factor (φ^R = 2) due to an increase in the protonated form of the catalyst at constant pL that necessitates a large offsetting normal fractionation factor (φ^T = 0.05). The solid black line assumes two normal fractionation factors: one reflecting the change in pK_a of the 2'OL ($1/\varphi^R$ = 0.2) and a second normal contribution of φ^T = 0.4

the vibrational modes in the ground state and transition state. For measurement of $^{18}k_{NUC}$, $^{18}k_{LG}$ and $^{18}k_{NPO}$, the appropriate site specifically enriched UpG molecules were synthesized and the KIEs measured by internal competition[18, 33, 34] (Fig. 3A). Previous KIE analyses on RNA and other phosphodiesters (see Table S1) provides a context for interpreting how the KIEs in terms of general TS structure.

A large normal value of $^{18}k_{LG}$ of 1.034(3) (standard errors in the last digit are shown in parenthesis) that is observed for specific base catalysis is attributable to advanced 5'O-P bond cleavage[18, 20, 33, 35, 36]. A similarly large $^{18}k_{LG}$ of 1.0272(1) is observed for base catalyzed transesterification of U-3'-*m*-nitrobenzylphosphate, which has a similarly unreactive leaving group (pK_a *ca*. 12) compared to the ribose 3'O (pKa *ca*. 13.4). Diester reactions with good leaving groups (*e.g.* nitrophenol, pK_a 7) react via early transition states with $^{18}k_{LG}$ values near unity[37, 38]. However, the $^{18}k_{LG}$ for the Zn^{2+}-catalyzed reaction is significantly less [1.015(2)] that the specific base reaction demonstrating a stiffer 5'O bonding environment in the TS due to metal ion catalysis.

The observed inverse $^{18}k_{NUC}$ value of 0.997(1) for the specific base reaction also reflects a late TS, and results from a large inverse contribution due of 0.980 due to formation of the 2'O-P bond[18, 19]. However, this contribution is partially offset by the large normal equilibrium isotope effect of *ca*. 1.024 due to loss of the 2'O-H stretching mode[18, 36, 39]. In contrast, normal $^{18}k_{NUC}$ values (1.02-1.04) are observed for reactions with early TSs in which nucleophilic attack is rate limiting (Table S1)[19, 38]. Thus, the observed inverse $^{18}k_{NUC}$ for the Zn^{2+}-catalyzed reaction is also consistent with a late TS.

The secondary ^{18}O effects on the non-bridging oxygens are near unity for both the specific base and metal ion catalyzed reactions. This result is consistent with both reactions proceeding by similar product-like, anionic TSs[20, 35]. For comparison, an inverse $^{18}k_{NPO}$ of 0.9904 is observed for acid catalysis of U-3'-*m*-nitrobenzyphosphate transesterification and 0.991(1) for RNA (Table S1), both of which are proposed to proceed via a stable phosphorane[20, 37]. Therefore, this mechanism is unlikely for Zn^{2+} catalysis. Formation of new vibrational modes give rise to normal equilibrium isotope effects on water coordination by metal ions[40, 41]. However, Mg^{2+} coordination to ATP was observed to result in an ^{18}O isotope effect no larger than 1.001[42]. A simple interpretation is that the non-bridging oxygen bonding environment is unchanged in the metal catalyzed reaction. However, the potential for multiple contributions to the observed $^{18}k_{NPO}$ effect that could be offsetting or complex obscures a simple interpretation.

The interpretation of KIE data with respect to TS structure are aided by DFT calculations examining the effect of different numbers of ions and different Zn^{2+} binding modes on TS structure. Recently, Chen et al described a set of alternative Zn^{2+} binding modes that were analyzed with respect to their effects on the predicted KIE values[43]. One or two metal ion interactions with the non-bridge phosphoryl oxygen or nucleophile involving either direct coordination, or interaction via coordinated water alone either gave no significant difference in observed KIEs or resulted in an early TS inconsistent with experimental data. A two metal ion mechanism is found to result in calculated KIEs that are consistent with the observed values reported here (Fig. 3C). In this model, the first Zn^{2+} ion (M_A) binds to the NPOs while the second ion, M_B, coordinates to the 5'O leaving group. M_A stabilizes accumulation of negative charge on the non-bridging oxygens allowing the formation of a TS that is more associative. Like the TS for specific

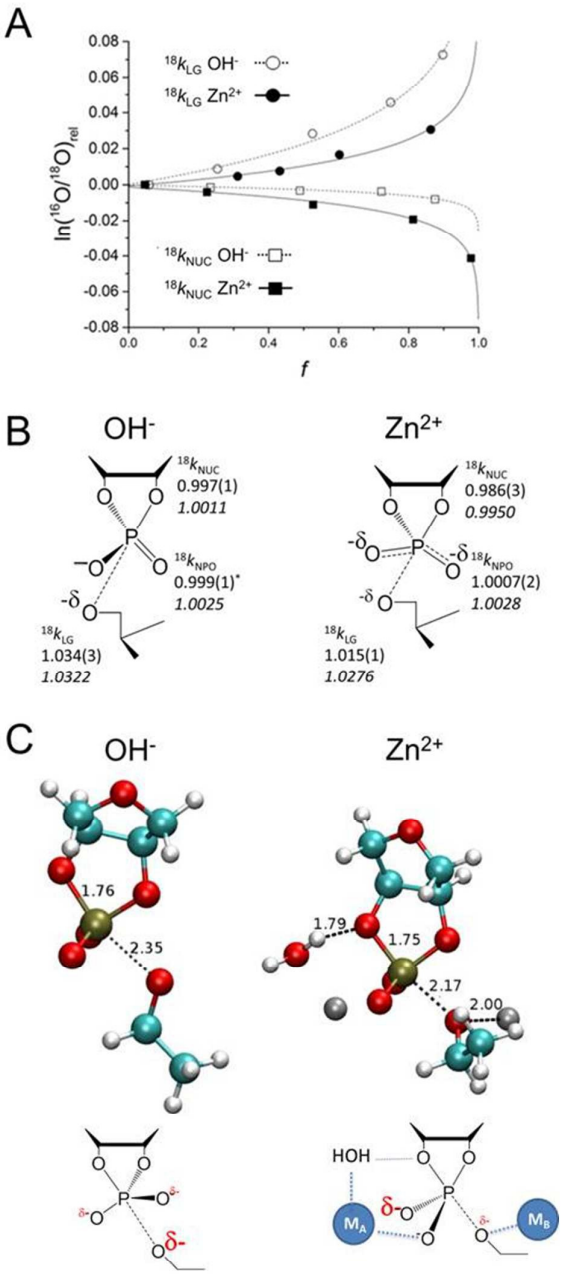

Fig. 3. Summary of KIE measurements for catalysis by specific base (OH-) and Zn(II). (**A**). Determination of ^{18}k values by fitting the ln(^{18}O/^{16}O) ratio in the unreacted substrate as a function of reaction progress (*f*) to Eq. 4 (ESI). (**B**). Summary of observed $^{18}k_{NUC}$, $^{18}k_{NPO}$ and $^{18}k_{LG}$ values. Standard errors in the last numeral are shown in parenthesis. The KIEs predicted from the TS models in part C are shown in italics. (**C**). TS models from DFT calculations for specific base catalysis and a model Zn^{2+}-catalyzed mechanism from Chen *et al*. 2015. Distances along the reaction coordinate for 2'O-P bond formation and 5'O-P bond cleavage are indicated in Angstroms. Two metal ion model for non-enzymatic catalysis by Zn^{2+}. As described in the text a two metal ion mechanism in which a metal ion interacts with the 5'O leaving group (M_A) and a second metal ion interacts via coordination to a non-bridging oxygen and via H-bonding to the 2'O (M_B)

base catalysis[18, 33, 36], the TS for Zn^{2+} catalysis involves advanced 2'O-P bonding, and this effect together with the M_AOH_2 mediated H-bond results in an observed $^{18}k_{NUC}$ that is overall inverse. H-bonding between the metal coordinated water and the nucleophile was proposed, however, 2'O-P bonding in the model is advanced and the 2'O acts only as an H-bond acceptor. Thus, only a small contribution to the observed SKIE would be expected[31, 32]. It may be inferred, however, that due to its proximity M_A may be pre-positioned to act as a specific base and facilitate transfer of the proton in a pre-equilibrium step.

Cleavage of a series of uridine-3-alkylphosphates by Zn^{2+} ions under the same reaction conditions used here for KIE measurements results in a significantly lower β_{LG} (−0.43 to −0.32)[22] compared to −1.28 reported for specific base catalysis[44]. The decrease in bond cleavage reflected in the shorter 5'O-P bond lengths in the specific base and Zn^{2+}-catalyzed models (2.35 versus 2.17 Å) (Fig. 3C) is consistent with the observed difference in charge accumulation indicated by the LFER results. In contrast to the late TS for RNA transphosphorylation, KIE, LFER data and computational results indicate that the uncatalyzed cyclization of 2-(hydroxypropyl)-4-nitrophenyl phosphate (HPPNP) and similar RNA models with activated leaving groups occur via early TSs. For these reactions there is little phosphorus-oxygen bond fission to the leaving group and minimal nucleophilic bond formation in the TS[18, 20, 37, 38]. Catalysis of HPPNP transphosphorylation by a dinuclear Zn^{2+} compound compared to specific base results in a larger $^{18}k_{LG}$ (1.0113(5) *versus* 1.0064(9)) and a smaller $^{18}k_{NUC}$ (1.0116(10) *versus* 1.0327(8)) (Table S1). The change in magnitude of these effects reflects an overall later TS with greater nucleophilic bond formation[45]. Recent computational simulations of HPPNP transphosphorylation are consistent with the KIE data and suggest a more associative TS[46], although one that is still early compared to the TS for RNA transphosphorylation demonstrated here. Nonetheless, a similar theme is observed relevant to enzyme mechanism. Transphosphorylation catalyzed by Zn^{2+} and Zn^{2+} complexes is accompanied by selection for an altered TS arising from the preferential stabilization of negative charge

Notes and references

1. J. K. Lassila, J. G. Zalatan and D. Herschlag, *Annu Rev Biochem*, 2011, **80**, 669-702.
2. S. C. Kamerlin, P. K. Sharma, R. B. Prasad and A. Warshel, *Q Rev Biophys*, 2013, **46**, 1-132.
3. D. E. Wilcox, *Chem Rev*, 1996, **96**, 2435-2458.
4. W. Yang, *Q Rev Biophys*, 2011, **44**, 1-93.
5. D. A. Hiller and S. A. Strobel, *Phil Trans Royal Soc*, 2011, **366**, 2929-2935.
6. G. Palermo, A. Cavalli, M. L. Klein, M. Alfonso-Prieto, M. Dal Peraro and M. De Vivo, *Acc Chem Res*, 2015, **48**, 220-228.
7. J. R. Morrow, T. L. Amyes and J. P. Richard, *Acc Chem Res*, 2008, **41**, 539-548.
8. M. Oivanen, S. Kuusela and H. Lonnberg, *Chem Rev*, 1998, **98**, 961-990.
9. H. Korhonen, N. H. Williams and S. Mikkola, *J Phys Org Chem*, 2013, **26**, 182-186.
10. R. Breslow and D. L. Huang, *Proc Natl Acad Sci U S A*, 1991, **88**, 4080-4083.
11. R. R. Breaker, G. M. Emilsson, D. Lazarev, S. Nakamura, I. J. Puskarz, A. Roth and N. Sudarsan, *RNA*, 2003, **9**, 949-957.
12. M. L. Zastrow and V. L. Pecoraro, *Coord Chem Rev*, 2013, **257**, 2565-2588.
13. H. Lonnberg, *Org Biomolec Chem*, 2011, **9**, 1687-1703.
14. H. Ikenaga and Y. Inoue, *Biochemistry*, 1974, **13**, 577-582.
15. D. M. Lilley, *Biochem Soc Trans*, 2011, **39**, 641-646.
16. C. M. Cuchillo, M. V. Nogues and R. T. Raines, *Biochemistry*, 2011, **50**, 7835-7841.
17. D. A. Usher, D. I. Richardson, Jr. and D. G. Oakenfull, *J Am Chem Soc*, 1970, **92**, 4699-4712.
18. M. E. Harris, Q. Dai, H. Gu, D. L. Kellerman, J. A. Piccirilli and V. E. Anderson, *J Am Chem Soc*, 2010, **132**, 11613-11621.
19. K. Y. Wong, H. Gu, S. Zhang, J. A. Piccirilli, M. E. Harris and D. M. York, *Angew Chem Int Ed Engl*, 2011, **5**, 823-826.
20. B. Gerratana, G. A. Sowa and W. W. Cleland, *J Am Chem Soc*, 2000, **122**, 12615-12621.
21. H. Korhonen, T. Koivusalo, S. Toivola and S. Mikkola, *Org Biomol Chem*, 2013, **11**, 8324-8339.
22. S. Mikkola, E. Stenman, K. Nurmi, E. Yousefi-Salakdeh, R. Stromberg and H. Lonnberg, *J. Chem. Soc., Perkin Trans*, 1999, **2**, 1619-1625.
23. P. F. Cook and W. W. Cleland, in *Enzyme Kinetics and Mechanism*, Garland Science, New York, 2007, ch. 9, pp. 253-324.
24. W. W. Cleland and A. C. Hengge, *Chem Rev*, 2006, **106**, 3252-3278.
25. W. W. Cleland, *Arch Biochem Biophys*, 2005, **433**, 2-12.
26. V. L. Schramm, *Acc Chem Res*, 2015, **48**, 1032-1039.
27. V. L. Schramm, *Annu Rev Biochem*, 2011, **80**, 703-732.
28. A. C. Hengge, *Biochim Biophys Acta*, 2015, **1854**, 1768-75.
29. L. I. Robins, E. J. Fogle and J. F. Marlier, *Biochim Biophys Acta*, 2015, **1854**, 1756-67.
30. P. F. Fitzpatrick, *Biochim Biophys Acta*, 2014, *Biochim Biophys Acta*, 2015, **1854**, 1746-55.
31. M. Q. Daniel, in *Isotope Effects In Chemistry and Biology*, CRC Press, 2005, Ch41, pp. 995-1018.
32. A. Virtanen, L. Polari, M. Valila and S. Mikkola, *J Phys Org Chem*, 2005, **18**, 385-397.
33. H. Gu, S. Zhang, K. Y. Wong, B. K. Radak, T. Dissanayake, D. L. Kellerman, Q. Dai, M. Miyagi, V. E. Anderson, D. M. York, J. A. Piccirilli and M. E. Harris, *Proc Natl Acad Sci U S A*, 2013, **110**, 13002-13007.
34. Q. Dai, J. K. Frederiksen, V. E. Anderson, M. E. Harris and J. A. Piccirilli, *J Org Chem*, 2007, **73**, 309-311.
35. A. C. Hengge, *FEBS Lett*, 2001, **501**, 99-102.
36. K. Y. Wong, H. Gu, S. Zhang, J. A. Piccirilli, M. E. Harris and D. M. York, *Angew Chem Int Ed Engl*, 2012, **51**, 647-651.
37. A. C. Hengge, *Acc Chem Res*, 2002, **35**, 105-112.
38. H. Chen, T. J. Giese, M. Huang, K. Y. Wong, M. E. Harris and D. M. York, *Chem Eur J*, 2014, **20**(44), 14336-43.
39. D. L. Kellerman, D. M. York, J. A. Piccirilli and M. E. Harris, *Curr Op Chem Biol*, 2014, **21c**, 96-102.
40. J. P. Hunt and H. Taube, *J. Chem. Phys.*, 1951, **19**, 602-609.
41. H. R. Hunt and H. Taube, *J. Phys. Chem.*, 1959, **63**, 124-125.
42. J. P. Jones, P. M. Weiss and W. W. Cleland, *Biochemistry*, 1991, **30**, 3634-3639.
43. H. Chen, J. A. Piccirilli, M. E. Harris and D. M. York, *Biochim Biophys Acta*, 2015, 1854(11):1795-800.
44. M. Kosonen, E. Youseti-Salakdeh, R. Stromberg and H. Lonnberg, *J Chem Soc, Perkin Trans 2*, 1997, 6, 2661-2666.
45. T. Humphry, S. Iyer, O. Iranzo, J. R. Morrow, J. P. Richard, P. Paneth and A. C. Hengge, *J Am Chem Soc*, 2008, **130**, 17858-17866.
46. H. Gao, Z. Ke, N. J. DeYonker, J. Wang, H. Xu, Z. W. Mao, D. L. Phillips and C. Zhao, *J Am Chem Soc*, 2011, **133**, 2904-2915.

1